Desalination and Water Treatment
www.deswater.com

doi: 10.5004/dwt.2021.27716

236 (2021) 285–299
October

Electrochemical degradation of tetracycline antibiotic with boron-doped diamond electrodes and effect of parameters on removal of reaction intermediates

Bahadır K. Körbahti*, Selin Alaca

Department of Chemical Engineering, Faculty of Engineering, Mersin University, Çiftlikköy Campus, 33343, Mersin, Turkey, Tel. +90 (324) 3610001 Ext. 17374; Fax: +90 (324) 3610032, emails: korbahti@mersin.edu.tr (B.K. Körbahti), selin.krky@gmail.com (S. Alaca)

Received 16 April 2021; Accepted 11 August 2021

ABSTRACT

Electrochemical degradation of tetracycline antibiotic and the effect of process parameters on removal of reaction intermediates was investigated with boron-doped diamond electrodes. The parameters of tetracycline concentration (200–1,000 mg/L), NaCl concentration (0–8 g/L), current density (4–20 mA/cm^2) and reaction temperature (25°C–45°C) were analyzed on tetracycline removal, chemical oxygen demand (COD) removal, intermediates removal, and energy consumption. The optimum values of the parameters were obtained by response surface methodology such as tetracycline concentration, 618 mg/L; NaCl concentration, 3.6 g/L; current density, 13.4 mA/cm^2, and reaction temperature, 36°C. Under optimum conditions, the removal efficiencies of tetracycline, COD, and intermediates were obtained as 98.7%, 98.2%, and 92.5%, respectively, with 78 kWh/kg COD$_r$ energy consumption. Electrochemical degradation rate of tetracycline antibiotic was higher in 10 min while intermediates started to produce after 2 min. The amount of the degradation products reached maximum in 15 min which then further oxidized and removed in high extent (≥97%) depending on reaction conditions. The removal of intermediates occurred at a much lower rate than tetracycline degradation.

Keywords: Electrochemical degradation; Boron-doped diamond; Optimization; Response surface methodology; Tetracycline

1. Introduction

Antibiotics are biologically active chemical substances that terminate or inhibit the growth of microorganisms and used as chemotherapeutic agents in humans, animals and plants for the treatment of microbial infections [1,2]. The annual consumption of antibiotics in human medicine, veterinary and agricultural purposes has been reported as thousands of tons worldwide [1–3].

Environmental concerns have been raised with the detection of significant amount of antibiotics in wastewater, surface water, drinking water, ground water, municipal sewage, soil, and sediments due to their extensive usage [1–5]. Antibiotics could be found in higher mg/L in hospital effluents, lower mg/L in municipal wastewater, and ng/L in sea, surface and groundwater [1,2]. Tetracycline antibiotics are being used for human medicine, veterinary and agricultural purposes. Most of the tetracyclines are released into environment by urine and feces from humans and animals after medication [4].

The accumulation of antibiotics in the ecosystems may produce toxic effects even at low concentrations [2]. In the presence of antibiotics and pharmaceuticals residues, the antibiotic resistant microorganisms may develop in the

---

* Corresponding author.

ecosystems in a long-term period [4,5]. Tetracycline antibiotics possess a wide range of antimicrobial activity against gram-positive and gram-negative bacteria that bind specifically to 30S ribosomes and appear to inhibit protein synthesis by preventing access of aminoacyl tRNA to the acceptor site on the mRNA-ribosome complex [4]. Halling-Sørensen [6] investigated the growth inhibiting effect of tetracycline antibiotics on two species of micro algae, *Microcystis aeruginosa* (freshwater cyanobacteria) and *Selenastrum capricornutum* (green algae) and the toxicity values (EC_{50}) were found as 0.09 and 2.2 mg/L, respectively. In the study of Xu et al. [7], the effects of tetracycline (TCY), and its degradation products of anhydrotetracycline (ATC) and epitetracycline (ETC) investigated on the growth, cell structure and algal cell oxidative stress of *Chlorella vulgaris*. 96 h-EC_{50} values of TCY, ATC and ETC on algal cells were 7.73, 5.96, and 8.42 mg/L, respectively. Furthermore, the acute toxicity of tetracycline on aquatic organisms *Daphnia magna*, *Danio rerio* and *Carassius auratus* were reported as 617.2 mg/L (48 h-EC_{50}), 406.0 mg/L (96 h-LC_{50}) and 322.8 mg/L (96 h-LC_{50}), respectively.

In practice different methods have been investigated using physical, chemical, biological and advanced oxidation processes for the removal of antibiotics and pharmaceuticals from wastewater and elimination of their toxicological effects [2,5,8,9]. It is known that most conventional treatment methods such as coagulation, flocculation, sedimentation and filtration were unsuccessful in removal of these compounds [1–5]. Due to the recalcitrant nature of the effluents containing the residues of antibiotics and pharmaceuticals, the applications of advanced oxidation processes (AOPs) and electrochemical processes emerge as alternative methods [2,5].

Advanced oxidation processes (AOPs) are defined as aqueous phase oxidation methods based on the production and use of $^{\bullet}OH$ radicals, which is a very powerful oxidant for the destruction of the organic pollutants ($E° = 2.8$ V) [4,5,10]. $^{\bullet}OH$ radicals are highly reactive species and react strongly with organic substances [4,10]. The most common AOPs for the production of $^{\bullet}OH$ radicals are Fenton process, photo-assisted Fenton process, photocatalysis using TiO_2 and UV radiation, combination of ozone and hydrogen peroxide, and hydrogen peroxide photolysis using UV light [10]. Although AOPs are capable in wastewater treatment, the disadvantages of the conventional AOPs were reported as relatively high costs, necessity of adding chemicals and complications of using UV light such as relatively short lifetime of UV light sources and high absorption coefficients of the water to be treated [4,10].

Electrochemical processes receive considerable attention in recent years for the treatment of antibiotics and pharmaceuticals in order to minimize and eliminate their biocide impact [11–13]. Pollutants can be removed by direct oxidation or indirect oxidation in electrochemical treatment processes. In direct oxidation the pollutants adsorb on the anode surface and destroy by direct electron transfer to the anode, and in indirect oxidation the pollutants degrade indirectly in the liquid bulk phase through electrochemically generated mediated oxidants [4,5,14–16]. The efficiency of direct oxidation mainly depends on the catalytic activity of electrode, whereas indirect oxidation depends on the diffusion rate of oxidants, solution pH and temperature [17,18]. Panizza et al. [19] reported that the small fraction of the organics is oxidized by direct electrolysis while complete mineralization is obtained with indirect electrolysis.

In electrochemical degradation of pharmaceuticals, Pt, boron-doped diamond (BDD), and Ti-based electrodes such as Ti/SnO_2, Ti/RuO_2, Ti/IrO_2, Ti/RuO_2-IrO_2 were reported recently [5,9,12,20–23]. Ti-based alloys and Pt anodes can achieve high tetracycline removal efficiency but not successful in complete removal of chemical oxygen demand (COD) and total organic carbon (TOC) [9,12,20,21]. On the other hand, BDD anode has better performances and almost completely mineralizes tetracycline and its intermediates, achieving high removal efficiency [8,9,20].

BDD is better than the anodes such as Pt, PbO_2, TiO_2, SnO_2, IrO_2, glassy carbon in electrochemical oxidation with its mechanical and chemical stability, good conductivity, inert surface, corrosion resistance, and increased mineralization rates in high current efficiency [24–27]. BDD electrodes are being investigated in electrochemical oxidation of organic compounds due to its superior properties [9,15,28]. BDD surface promotes the production and the adsorption of $^{\bullet}OH$ radicals by oxidation of water molecules [Eq. (1)]. In the presence of organic compound, $^{\bullet}OH$ radicals involve in nonselective indirect oxidation of organic compounds (R) and their reaction intermediates (RO) may result in complete mineralization [Eqs. (2) and (3)] [15,29].

$$\mathrm{BDD} + \mathrm{H_2O} \rightarrow \mathrm{BDD}\left[{}^{\bullet}\mathrm{OH}\right] + \mathrm{H^+} + \mathrm{e^-} \tag{1}$$

$$\mathrm{BDD}\left[{}^{\bullet}\mathrm{OH}\right] + \mathrm{R} \rightarrow \mathrm{BDD} + \mathrm{RO} + \mathrm{H^+} + \mathrm{e^-} \tag{2}$$

$$\mathrm{BDD}\left[{}^{\bullet}\mathrm{OH}\right] + \left\langle \mathrm{R/RO} \right\rangle \rightarrow \mathrm{BDD} + \mathrm{CO_2} + \mathrm{H_2O} \tag{3}$$

The electrochemical production of $^{\bullet}OH$ radicals directly from water with an anodic reaction using BDD anode can be defined as electrochemical advanced oxidation process [10,30]. There is no necessary addition of chemical substances in the production of $^{\bullet}OH$ radicals using BDD anode. Besides, this process avoids the disadvantages of conventional AOPs and can be operated at reasonable costs depending on the power required for the electrochemical oxidation [10].

Indirect oxidation initiates as well with Cl_2 gas evolution on the anode when NaCl used as electrolyte [Eq. (4)]. NaCl is commonly used electrolyte in order to increase the conductivity and to produce secondary oxidants for indirect oxidation [2]. Hydrolysis and ionization reactions occur in the solution [Eqs. (5)–(8)] [15,28,31–35], and anodically generated redox reagents of $HOCl/OCl^-$ can indirectly oxidize the organic compounds [31,33,35]. Fig. 1 demonstrates the degradation of tetracycline antibiotic with electrochemically generated $^{\bullet}OH$ radicals using BDD electrode, and $HOCl/OCl^-$ redox reagents produced by the electrolysis of treated solution with NaCl supporting electrolyte. $HOCl/OCl^-$ distribution in solution depends on the pH [32]. Brillas and Martínez-Huitle [28] was indicated that Cl_3^- ion forms in very low concentrations up to pH 4.0, while the species

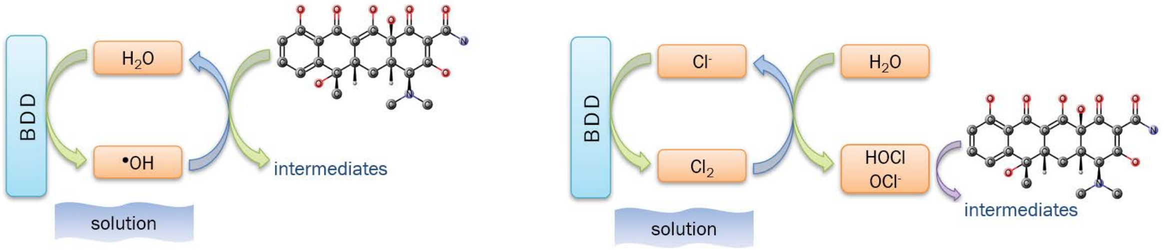

Fig. 1. Degradation of tetracycline antibiotic with electrochemically generated •OH radicals and HOCl/OCl^- redox reagents.

are Cl_2 until pH 3.0, and HOCl in the pH range 3–8 and OCl^- for pH > 8.0.

$$2Cl^- \rightarrow Cl_2 + 2e^- \tag{4}$$

$$Cl_2 + H_2O \rightleftharpoons HOCl + H^+ + Cl^- \tag{5}$$

$$HOCl \rightleftharpoons H^+ + OCl^- \tag{6}$$

$$6OCl^- + 3H_2O \rightarrow 2ClO_3^- + 4Cl^- + 6H^+ + \frac{3}{2}O_2 + 6e^- \tag{7}$$

$$OCl^- + H_2O + 2e^- \rightarrow Cl^- + 2OH^- \tag{8}$$

In this study, the electrochemical degradation of tetracycline antibiotic with BDD electrodes was investigated. Central composite design (CCD) was applied for the design of experiments and the operating parameters were optimized by response surface methodology (RSM). The overall amount of electrochemical degradation intermediates was evaluated with component mass balance in high-performance liquid chromatography (HPLC). Reaction intermediates were formed, then further oxidized and almost completely removed depending on reaction conditions even at very high tetracycline concentrations.

2. Materials and methods

2.1. Chemicals and materials

Tetracycline hydrochloride ($C_{22}H_{25}N_2O_8Cl$) (Sigma-Aldrich, Germany), mercury sulfate (Merck, Germany), sodium chloride (Merck, Germany), and acetonitrile (Merck, Germany) were received in extra pure grade. Double distilled water was produced with resistivity 18.2 MΩ cm at 25°C and TOC < 5 ppb using water still (GFL-2008) and Millipore Simplicity® UV ultrapure water system. Merck Spectroquant® 14541 COD cell tests were used for COD analysis.

2.2. Experimental set-up and procedure

The batch system was equipped with heating/cooling jacketed DURAN® glass electrochemical reactor (Rettberg), programmable DC power supply (Ametek Sorensen XFR 60-46), refrigerated circulating water bath with thermostat control (Lauda RE 620S), peristaltic pump (Cole Parmer Masterflex® RZ-77924-60), mechanical mixer (Heidolph RZR 2021) and thermometer. DIACHEM® boron-doped diamond (Nb/BDD) electrode (CONDIAS) with 260 cm^2 surface area were used as anode and cathode. The reaction volume was 600 mL and mechanically stirred at 500 rpm. Aliquots were taken from the reaction medium at regular intervals for pH measurements, HPLC and COD analysis.

2.3. Analytical procedure

HPLC analysis were performed using Inertsil ODS-3 column (5 µm, 4.6 mm × 250 mm) in a Shimadzu Prominence LC-20AD Liquid Chromatography. Gradient mobile phase was acetonitrile and water (50/50) (v/v) at a flow rate of 1.5 mL/min. UV/Vis detection wavelength of tetracycline antibiotic was at 254 nm. Column temperature was set at 40°C. Injection volume was 30 µL. The regression coefficient (R^2) for the calibration curve of tetracycline antibiotic was 0.9995. pH was measured with WTW inoLab BNC720 pH meter/conductivity meter. Merck Spectroquant® TR 420 thermoreactor and Nova 60 photometer were used for the COD analysis. In order to prevent the interference of Cl^- ions, the aliquots were pretreated with required amounts of $HgSO_4$ before COD analysis according to COD correction procedure [36,37].

2.4. Design of experiments

Response surface methodology is mathematical and statistical method for design of experiments, building models, evaluating the effects of parameters, and searching optimum conditions to predict the responses [31,38,39]. In response surface methodology, the parameters (factors) are related to the responses by linear or quadratic models [31,38,39]. CCD is a second-order design that provide very well predictions for the design space. In this study, CCD with 4 parameters at 5 levels was coded between the limits of –2 and +2 for tetracycline concentration (200–1,000 mg/L), current density (4–20 mA/cm^2), NaCl concentration (0–8 g/L), and reaction temperature (25°C–45°C). Experimental runs were designed in two blocks with 16 factorial, 8 axial, 6 center and additional 8 axial points and carried out in randomized order. The adequacy of the response surface models was analyzed by the regression coefficients of R^2 and R^2_{adj}. The statistical significance was checked by the F-values, P-values, and signal/noise (s/n) ratio [31].

3. Results and discussions

The effect of tetracycline concentration (A), NaCl concentration (B), current density (C) and reaction temperature

(*D*) were investigated on electrochemical degradation of tetracycline antibiotic with BDD electrodes. The experimental data were processed using Design-Expert 12 to obtain the interaction between the parameters and the responses as given in Eq. (9).

$$y = \beta_0 + \sum_{i=1}^{k}\beta_i x_i + \sum_{i=1}^{k}\beta_{ii} x_i^2 + \sum_{i}\sum_{<j=2}^{k}\beta_{ij} x_i x_j \tag{9}$$

The main effects and significant interactions of the independent variables on the dependent variables were investigated using Pareto chart in two-level 24 full factorial design. Pareto chart is a graphical tool used to manage model selection for two-level factorial designs. In the study, Design-Expert 12 was used for the analysis of each variable effect on the designated response. Firstly, half-normal plot (not shown) used to select effects that were obviously larger than the others and then Pareto chart in Fig. 2 used to see if it belongs with error or may be a true effect. The vertical axis shows the *t*-value of the absolute effects. This dimensionless statistic scales the effects in terms of standard deviations and computed by dividing the numerical effect by its standard error [40,41]. Two limit lines as Bonferroni limit line and *t*-value limit line also seen in Fig. 2. The highest limit is based on the Bonferroni *t*-value (more conservative *t*-value) and the lower limit is based on standard *t*-value for individual effects tests. Selected effects that are above the Bonferroni limit are almost certainly important and should be left in the model. Effects that are above the *t*-value limit are possibly important. Effects that below the *t*-value limit can be selected to support hierarchy [40,41].

In Fig. 2, the effects from largest to smallest (left to right) were selected until all other effects fall below the Bonferroni limit and *t*-value limit. Contribution percentage of main effects and significant interactions in Pareto analysis can be seen in Table 1. The most important factor was tetracycline concentration (*A*) for all dependent variables, and less important factors were NaCl concentration (*B*) for tetracycline removal, COD removal, mass transfer coefficient and J/J^o_{lim} ratio; current density (*C*) for tetracycline removal and COD removal; and reaction temperature (*D*) for average quantification of electrochemical oxidation intermediates and by-products (EOX) and energy consumption.

The important factors and significant interactions above the *t*-value limit line were found as: tetracycline concentration (*A*), reaction temperature (*D*) and tetracycline concentration × reaction temperature (*AD*) for tetracycline removal; tetracycline concentration (*A*), NaCl concentration (*B*) and current density (*C*) for EOX; tetracycline concentration (*A*), current density (*C*), reaction temperature (*D*) and tetracycline concentration × current density (*AC*) for COD removal; tetracycline concentration (*A*), current density (*C*) and reaction temperature (*D*) for mass transfer coefficient; tetracycline concentration (*A*) and reaction temperature (*D*) for J/J^o_{lim} ratio; and tetracycline concentration (*A*), NaCl concentration (*B*), current density (*C*), tetracycline concentration × NaCl concentration (*AB*), tetracycline concentration × current density (*AC*) and NaCl concentration × current density (*BC*) for energy consumption.

The second-order response surface models were obtained in Eqs. (10)–(15), and the statistical significance checked by the analysis of variance (ANOVA). In Eqs. (10)–(15), y_{TCY}, y_{EOX}, y_{COD}, y_{km}, $y_{J/J^o_{\text{lim}}}$, and y_{EC} are the responses of tetracycline removal, average quantification of electrochemical oxidation intermediates and by-products, COD removal, mass transfer coefficient, J/J^o_{lim}, and energy consumption, respectively.

$$\begin{aligned} y_{\text{TCY}} = {} & 0.038989A + 2.90669B + 3.42839C + 3.68706D + 2.68594 \\ & \times 10^{-3}AB + 1.30859\times 10^{-3}AC - 1.51562\times 10^{-3}AD \\ & - 0.073203BC - 0.015812BD - 0.054656CD - 4.47610 \\ & \times 10^{-6}A^2 - 0.46741B^2 - 0.093212C^2 - 0.026397D^2 - 6.08649 \end{aligned} \tag{10}$$

$$\begin{aligned} y_{\text{EOX}} = {} & -5.86340\times 10^{-4}A + 2.58137\times 10^{-3}B - 0.039210C \\ & - 0.024684D - 6.07812\times 10^{-6}AB - 1.92969\times 10^{-6}AC \\ & + 2.00625\times 10^{-6}AD + 1.05469\times 10^{-4}BC + 1.99375 \\ & \times 10^{-4}BD + 1.26562\times 10^{-4}CD + 4.67543\times 10^{-7}A^2 \\ & - 5.45343\times 10^{-6}B^2 + 1.30195\times 10^{-3}C^2 \\ & + 2.86892\times 10^{-4}D^2 + 1.00663 \end{aligned} \tag{11}$$

$$\begin{aligned} y_{\text{COD}} = {} & -0.011780A + 12.07680B + 10.36859C + 4.88335D \\ & - 3.70312\times 10^{-4}AB + 3.13047\times 10^{-3}AC + 3.65625 \\ & \times 10^{-4}AD + 0.10586BC - 0.14269BD + 0.068781CD \\ & - 5.30043\times 10^{-5}A^2 - 0.89093B^2 - 0.52479C^2 \\ & - 0.081313D^2 - 73.45841 \end{aligned} \tag{12}$$

$$\begin{aligned} y_{k_m\times 10^5} = {} & 2.21462\times 10^{-3}A + 0.42365B + 0.43440C + 0.27222D \\ & - 6.86812\times 10^{-5}AB - 4.88139\times 10^{-5}AC + 3.45693 \\ & \times 10^{-5}AD + 4.07392\times 10^{-3}BC - 2.54603\times 10^{-3}BD \\ & - 3.66265\times 10^{-4}CD - 2.57277\times 10^{-6}A^2 - 0.037347B^2 \\ & - 0.015199C^2 - 4.00977\times 10^{-3}D^2 - 7.81025 \end{aligned} \tag{13}$$

$$\begin{aligned} y_{J/J^o_{\text{lim}}} = {} & -7.99301\times 10^{-3}A - 0.76911B - 0.45166C - 0.30268D \\ & + 1.83473\times 10^{-4}AB - 9.19212\times 10^{-5}AC - 7.07628 \\ & \times 10^{-5}AD - 0.010140BC + 5.55310\times 10^{-3}BD - 1.24006 \\ & \times 10^{-3}CD + 7.86747\times 10^{-6}A^2 + 0.064562B^2 + 0.025607C^2 \\ & + 5.26779\times 10^{-3}D^2 + 12.78077 \end{aligned} \tag{14}$$

$$\begin{aligned} y_{\text{EC}} = {} & -0.31664A - 49.69991B + 14.39273C + 2.95963D + 9.43906 \\ & \times 10^{-3}AB - 0.016018AC + 3.85625\times 10^{-4}AD - 0.63977BC \\ & + 0.060437BD - 0.083031CD + 2.61232\times 10^{-4}A^2 + 4.93114B^2 \\ & + 0.34992C^2 - 0.032900D^2 + 141.25559 \end{aligned} \tag{15}$$

The second-order models are significant for tetracycline removal, EOX, COD removal, k_m, and J/J^o_{lim} according to model *F*-values of 5.50, 4.46, 8.62, 4.70, 4.06 and 13.74, respectively. *P*-values < 0.05 indicate the model terms are significant and s/n ratio >4 is desirable for adequate precision. In Table 2, s/n ratios of 9.554, 9.604, 12.521, 8.808, 6.969 and 13.988 indicate the significance for the quadratic models

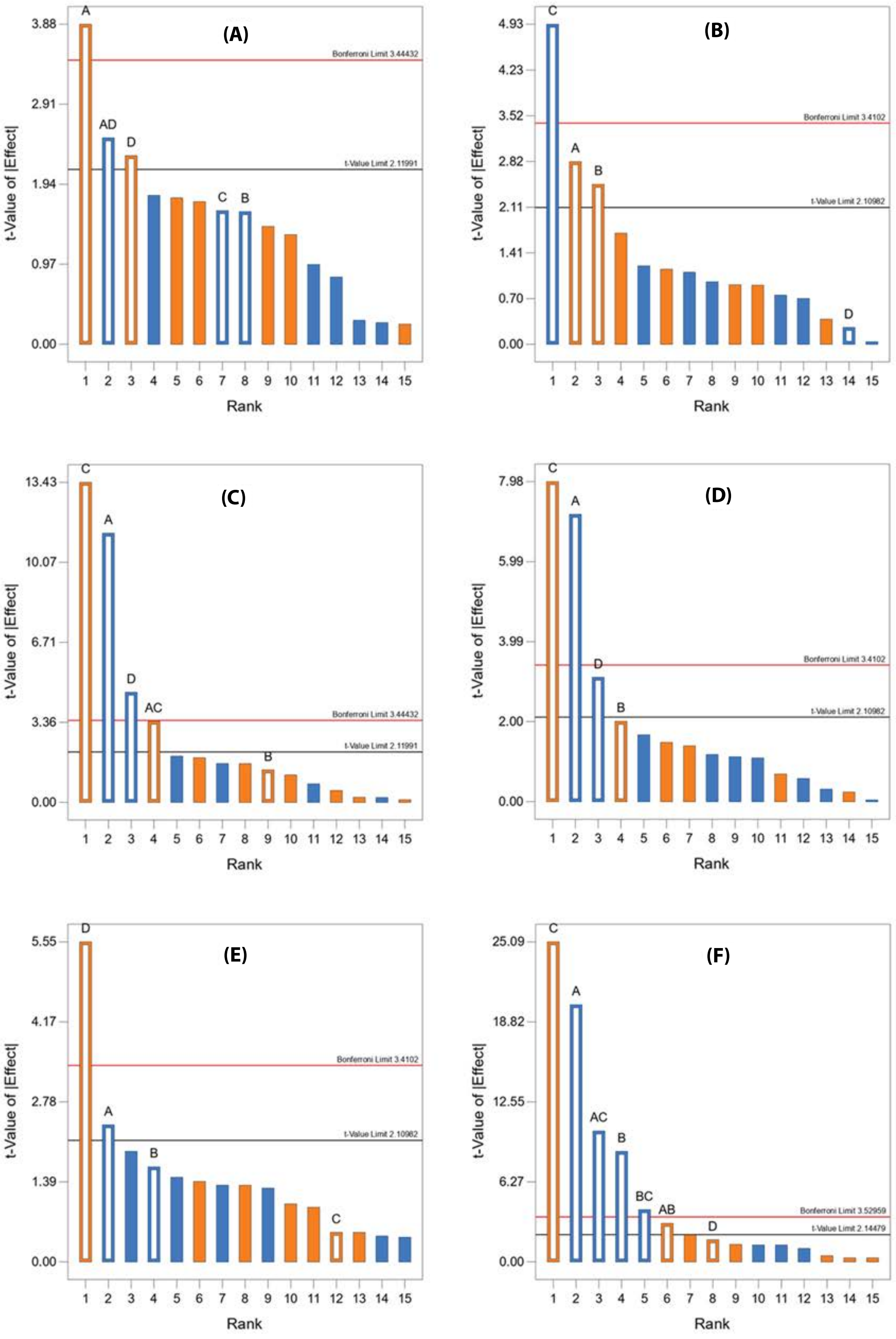

Fig. 2. Pareto chart of the main effects and significant interactions on dependent variables (🟧 positive effects, 🟦 negative effects): (A) tetracycline removal, (B) average quantification of electrochemical oxidation intermediates and by-products (EOX), (C) COD removal, (D) mass transfer coefficient (k_m), (E) $J/J^o_{\lim}$ ratio, and (F) energy consumption.

in 95% confidence interval for the design space. R^2 and R^2_{adj} regression coefficients were satisfactorily correlated the predicted and the actual values of the responses. The contour plots in Figs. 3, 6–10 were sketched using the quadratic models in Eqs. (10)–(15).

Tetracycline removal was obtained between 87.3%–100.0% with standard deviation of 3.73%. In Fig. 3, complete tetracycline removal was achieved in the regions between 2.3–6.5 g/L NaCl, 35°C–43°C reaction temperature, and 4.9–12.4 mA/cm^2 current density. In the study, degradation of tetracycline antibiotic resulted in tetracycline abatement and COD reduction by weakly adsorbed hydroxyl radicals at boron-doped diamond anode surface and via generated redox reagents of $HOCl/OCl^-$ in the bulk phase. The concentration of $HOCl/OCl^-$ oxidants increases in the reaction medium with increasing the electrolyte concentration and current density. However, secondary reactions of gas evolution, electrolyte decomposition, and intermediates formation also occur in the mineralization of organic compounds that results in removal efficiency decrease and current efficiency loss [22]. In electrochemical processes, current density is the most influential parameter for controlling mass transfer and the reaction rate [31]. The electrochemical degradation efficiency increases by the increase in current density, however secondary reactions may consume the applied current at very high cell voltages [22,42]. This may also result in significant iR drop, current efficiency loss and removal efficiency decrease.

In direct or indirect electrochemical oxidation intermediates form before complete mineralization even without NaCl [16]. In the study, while antibiotic degradation rate was higher in the first 10 min, it was determined from HPLC analysis that intermediates started to form in the reaction medium after 2 min. The abatement of tetracycline antibiotic and the formation of intermediates during the electrochemical degradation can be seen in Fig. 4. Tetracycline peak at $t = 0$, and intermediates at $t = 120$ min is shown in Fig. 4 (inset). In the HPLC chromatograms, the intermediate products started to appear with retention time shorter than that of tetracycline [43,44] and no additional peaks were observed as the electrochemical oxidation proceeds. This HPLC result indicate that the degradation products have higher polarity than tetracycline since they elute faster from the non-polar chromatographic column [43,44]. The intensity of tetracycline peak decreased with reaction time, whereas the intensity of intermediates peaks increased and reached a maximum in 15 min. Then the intensity of the peaks decreased and the intermediate products formed in the reaction medium were almost completely removed with advanced electrochemical oxidation depending on the reaction conditions. Similar results were obtained under different operating conditions. The overall amount of the intermediates was calculated from the areas of the peaks formed with retention time shorter than tetracycline peak.

Comninellis and Chen [16] and Panizza and Cerisola [25] reported that COD decreases linearly and large amounts of intermediates form at high concentrations of organic compounds or low current densities. The effect of the parameters on the removal of reaction intermediates can be seen in Fig. 5. The lowest tetracycline concentration of 200 mg/L resulted in the formation of higher amount of intermediates. The initial formation rate of intermediates were decreased as the tetracycline concentration increased. The amount of intermediates increased with increasing NaCl supporting electrolyte concentration. This behavior can be attributed to the formation of $HOCl/OCl^-$ oxidants in the bulk phase, which promote the formation of intermediates. In addition, the initial formation rate of intermediates increased with increasing NaCl concentration. The lowest amount of intermediates was obtained in the absence of NaCl electrolyte. The lowest initial formation rate was obtained at 4 mA/cm^2 current density, while the highest intermediate amount was obtained at 4 mA/cm^2. Also, the removal time of the intermediates was prolonged at the lowest current density of 4 mA/cm^2. The removal of reaction intermediates may be considered as mass transfer-controlled reaction when current density is greater than 4 mA/cm^2 due to the small change in the initial formation rate of intermediates above 4 mA/cm^2. The amount of intermediates decreased with increasing the current density. This result also supports that current density is the most effective parameter in electrochemical processes. While the highest amount of intermediates was

Table 1
Contribution of main effects and significant interactions in Pareto analysis: (A) tetracycline removal, (B) average quantification of electrochemical oxidation intermediates and by-products (EOX), (C) COD removal, (D) mass transfer coefficient (k_m), (E) J/J^o_{lim} ratio, (F) energy consumption

Term	Contribution of main effects and significant interactions (%)					
	(A)	(B)	(C)	(D)	(E)	(F)
A-Tetracycline concentration	24.2563*	3.79754*	23.7024*	13.8289*	2.83907*	28.4733*
B-NaCl concentration	4.16157	2.91508*	0.345642	1.08098	1.36603	5.25006*
C-Current density	4.22597	11.6738*	33.5001*	17.1559*	0.132459	44.0993*
D-Reaction temperature	8.42224*	0.0324125	3.97222*	2.59382*	15.4804*	0.212682
AB						0.640532*
AC			2.15434*			7.37832*
AD	10.0949*					
BC						1.17702*

(*) above *t*-value limit

Table 2
ANOVA results of the quadratic models

Source	SS	DF	MS	*F*-value	*P*-value
Tetracycline removal[a]					
Model	389.16	14	27.80	5.50	0.0002
Residual	111.28	22	5.06		
Lack of fit	111.28	17	6.55		
Pure error	0.000	5	0.000		
Average quantification of intermediates and by-products[b]					
Model	0.034	14	2.453×10^{-3}	4.46	0.0009
Residual	0.012	22	5.497×10^{-4}		
Lack of fit	0.012	17	6.879×10^{-4}	8.62	0.0129
Pure error	3.991×10^{-4}	5	7.982×10^{-5}		
COD removal[c]					
Model	5,810.90	14	415.06	8.62	<0.0001
Residual	1,058.94	22	48.13		
Lack of fit	1,057.54	17	62.21	221.62	<0.0001
Pure error	1.40	5	0.28		
Mass transfer coefficient[d]					
Model	3.52	14	0.25	4.70	0.0006
Residual	1.18	22	0.054		
Lack of fit	1.14	17	0.067	8.92	0.0119
Pure error	0.038	5	7.527×10^{-3}		
J/J^{o}_{lim} ratio[e]					
Model	11.15	14	0.80	4.06	0.0017
Residual	4.31	22	0.20		
Lack of fit	4.29	17	0.25	53.38	0.0002
Pure error	0.024	5	4.725×10^{-3}		
Energy consumption[f]					
Model	73,923.76	14	5,280.27	13.74	<0.0001
Residual	8,455.89	22	384.36		
Lack of fit	8,418.59	17	495.21	66.38	<0.0001
Pure error	37.30	5	7.46		

[a] $R^2 = 0.7776$, $R^2_{\text{adj}} = 0.6361$, s/n = 9.554; [b] $R^2 = 0.7396$, $R^2_{\text{adj}} = 0.5739$, s/n = 9.604; [c] $R^2 = 0.8459$, $R^2_{\text{adj}} = 0.7478$, s/n = 12.521; [d] $R^2 = 0.7493$, $R^2_{\text{adj}} = 0.5898$, s/n = 8.808; [e] $R^2 = 0.7212$, $R^2_{\text{adj}} = 0.5437$, s/n = 6.969; [f] $R^2 = 0.8974$, $R^2_{\text{adj}} = 0.8320$, s/n = 13.988

obtained at 25°C, the amount of intermediates decreased and the removal efficiency increased with the increase of the reaction temperature.

The nature and the amounts of intermediates depends on the process conditions and the local concentration of •OH radicals on BDD anode surface [15,16]. The oxidation of tetracycline may occur at any ring and degradation reaction include electron transfer, hydroxylation, opening reactions and cleavage of the central carbon [45,46]. •OH radicals attack three functional groups on tetracycline with relatively high electron density such as double bonds, amine group and phenolic group resulting in the formation of primary, secondary and tertiary intermediate compounds which are then undergo anodic oxidation at lower reaction rates to short-chain carboxylic acids (oxalic acid, formic acid, carbamic acid and 2-oxo-malonic acid), CO_2 and H_2O [8,21,30,43,46–48]. Electrochemical advanced oxidation reactions produce very complicated reaction pathways for different anode materials and different intermediate compounds may be generated in different pathways. Therefore, further detailed investigations require for the mechanisms of intermediates production with electrochemical oxidation of tetracycline [8,21,30].

In order to determine the average quantification of intermediates even without the identification of the degradation products, a dimensionless quantity EOX parameter in Eq. 16 was used with component mass balance in HPLC chromatograms obtained for aliquots collected at different time intervals, which was developed in our previous studies [22,23]. EOX value was obtained by dividing

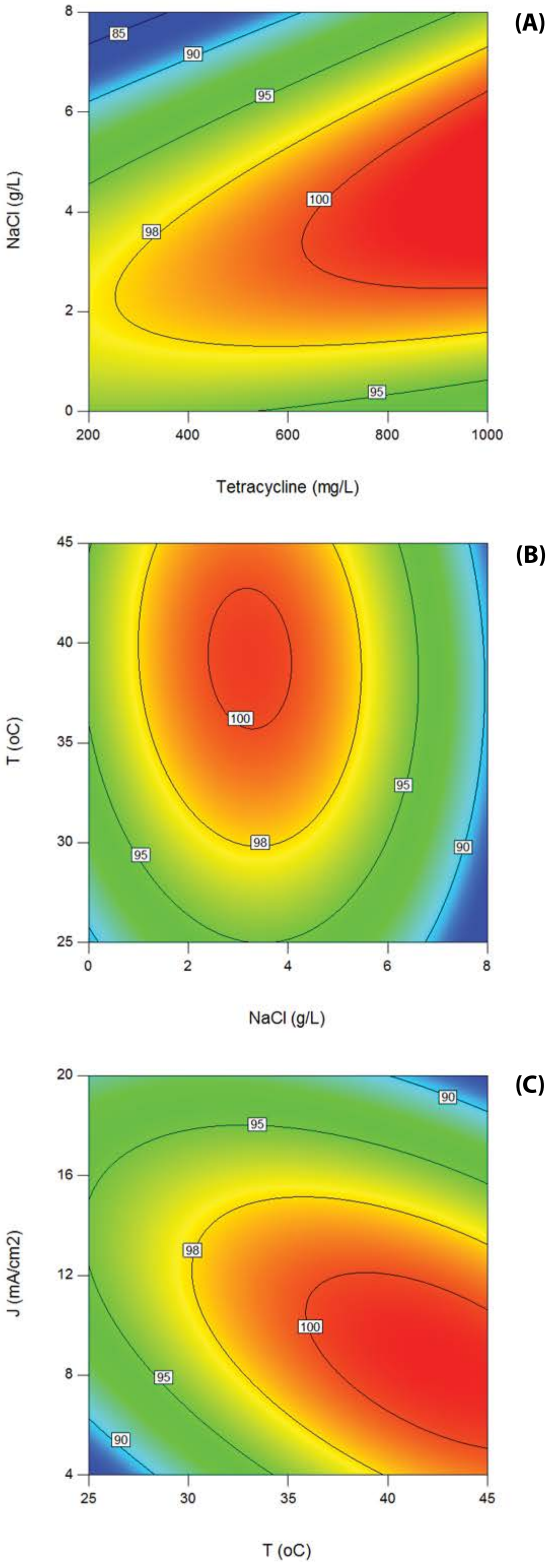

Fig. 3. Effect of parameters on tetracycline removal: (A) effect of tetracycline concentration and NaCl concentration (J = 12 mA/cm^2; T = 35°C), (B) effect of NaCl concentration and reaction temperature ([TCY] = 600 mg/L; J = 12 mA/cm^2), and (C) effect of reaction temperature and current density ([TCY] = 600 mg/L; [NaCl] = 4 g/L).

the area of HPLC chromatogram of intermediates and by-products at time t (t = 120 min) by the total area of HPLC chromatogram at initial time (t = 0), and then dividing the result by the total reaction time in stirred batch electrochemical reactor.

$$\text{EOX} = \frac{1}{\tau_R}\int_0^t \left(\frac{C(t)}{C_0}\right)dt \quad (16)$$

EOX value was defined between 0 and 1 (0 ≤ EOX ≤ 1) that shows the degree of mineralization. EOX = 0 means that no organic compounds remained in the reaction medium with complete mineralization, whereas EOX = 1 means that organic compounds remained in the reaction medium as intermediates and by-products without mineralization [22,23]. EOX values were calculated between 0.0604–0.2566 with standard deviation of 0.0358. In Fig. 6, the lowest EOX values were found in the regions between 390–760 mg/L tetracycline concentration, 34°C–42°C reaction temperature, and 12.4–14.7 mA/cm^2 current density.

COD removal increased due to the increase of electrogenerated HOCl/OCl$^-$ oxidants with increasing NaCl concentration. Degradation efficiency also increased with increasing current density that provided the production of $^\bullet$OH radicals at boron-doped diamond anode and increased production rate of HOCl/OCl$^-$ oxidants in the bulk phase. COD removal was obtained between 49.7%–99.2% with standard deviation of 14.08%. In Fig. 7, complete COD removal was obtained in the regions between 3.2–6.0 g/L NaCl, 29°C–38°C reaction temperature, and 12.8–15.8 mA/cm^2 current density. In electrochemical treatment of organic compounds in aqueous solutions, increase in current density increases the degradation of organic compounds, COD removal, and also energy consumption [25,26,49–51].

The mineralization reaction rate is independent of the nature of the organic compound [16]. Therefore, mass transfer coefficient could be defined by mass balance under mass transfer control with convective diffusion (Eq. 17) [22,34,52–54].

$$x_{\text{SBER}} = 1 - e^{\frac{-k_m A_e t}{V_R}} \quad (17)$$

Mass transfer coefficients were calculated between 0.220 × 10^{-5}–1.543 × 10^{-5} with standard deviation of 0.369 × 10^{-5} which are close or higher to those reported in the literature for the electrochemical degradation of tetracycline on BDD electrode [20]. In Fig. 8, the highest mass transfer coefficients were achieved in the regions between 265–715 mg/L tetracycline concentration, 29°C–40°C reaction temperature, and 2.8–6.6 g/L NaCl, 10.7–16.2 mA/cm^2 current density. The results in these regions indicated that batch electrochemical reactor with BDD electrode was operated under mass transfer control via convective diffusion.

The limiting current density (J^o_{lim}) can be expressed for the mineralization of organic compounds under hydrodynamic conditions in electrochemical reactors [Eq. (18)] [14–16]. The operating regimes such as current-controlled or mass transfer-controlled can be defined by J/J^o_{lim} ratio. In current-controlled processes $J/J^o_{\text{lim}} < 1$, while in mass transfer-controlled processes $J/J^o_{\text{lim}} > 1$ [14–16].

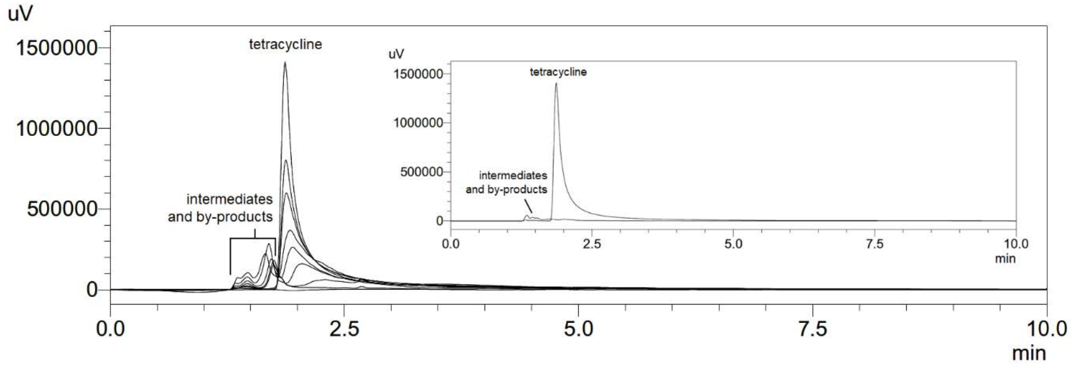

Fig. 4. HPLC chromatogram of a sample in electrochemical degradation of tetracycline antibiotic with BDD electrodes ([TCY] = 600 mg/L; [NaCl] = 4 g/L; J = 12 mA/cm^2; T = 35°C).

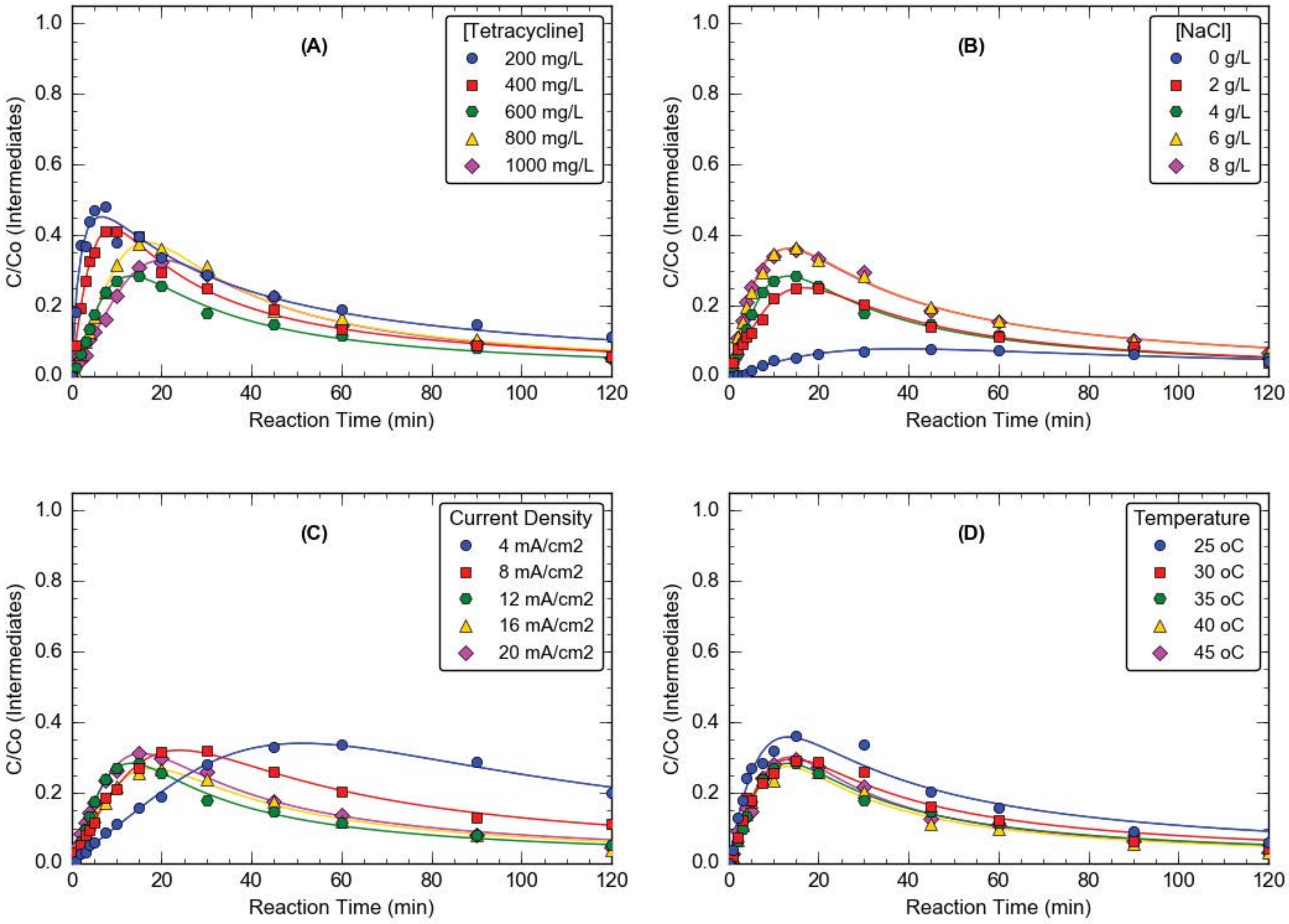

Fig. 5. Effect of parameters on removal of reaction intermediates: (A) effect of tetracycline concentration ([NaCl] = 4 g/L; J = 12 mA/cm^2; T = 35°C), (B) effect of NaCl concentration ([TCY] = 600 mg/L; J = 12 mA/cm^2; T = 35°C), (C) effect of current density ([TCY] = 600 mg/L; [NaCl] = 4 g/L; T = 35°C), and (D) effect of reaction temperature ([TCY] = 600 mg/L; [NaCl] = 4 g/L; J = 12 mA/cm^2).

$$J^o_{\lim} = 4Fk_m\text{COD}_o \tag{18}$$

$J/J^o_{\lim}$ values were obtained between 0.58–3.14 with standard deviation of 0.68 in Fig. 9. Many intermediates form in the electrolysis under current control according to the electrolysis under mass transfer control [14–16]. Therefore, the parameters were optimized in this study for mass transfer-controlled regime in order to reduce the amount of intermediates.

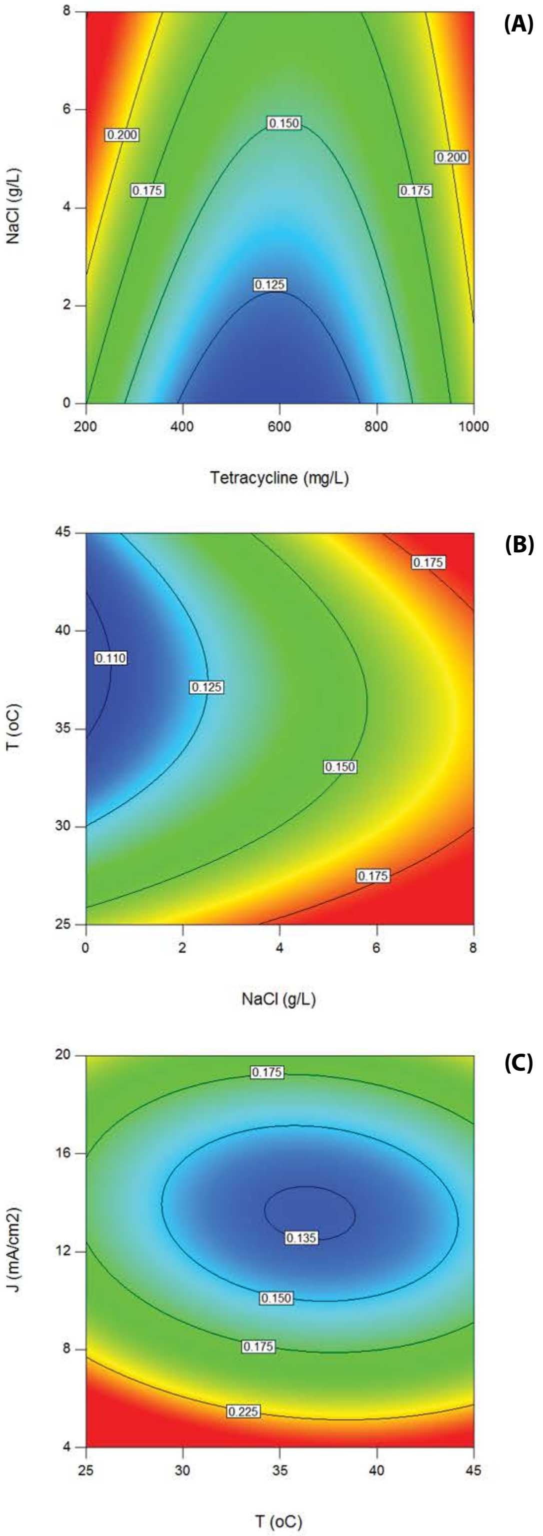

Fig. 6. Effect of parameters on average quantification of electrochemical oxidation intermediates and by-products (EOX): (A) effect of tetracycline concentration and NaCl concentration (J = 12 mA/cm^2; T = 35°C), (B) effect of NaCl concentration and reaction temperature ([TCY] = 600 mg/L; J = 12 mA/cm^2), and (C) effect of reaction temperature and current density ([TCY] = 600 mg/L; [NaCl] = 4 g/L).

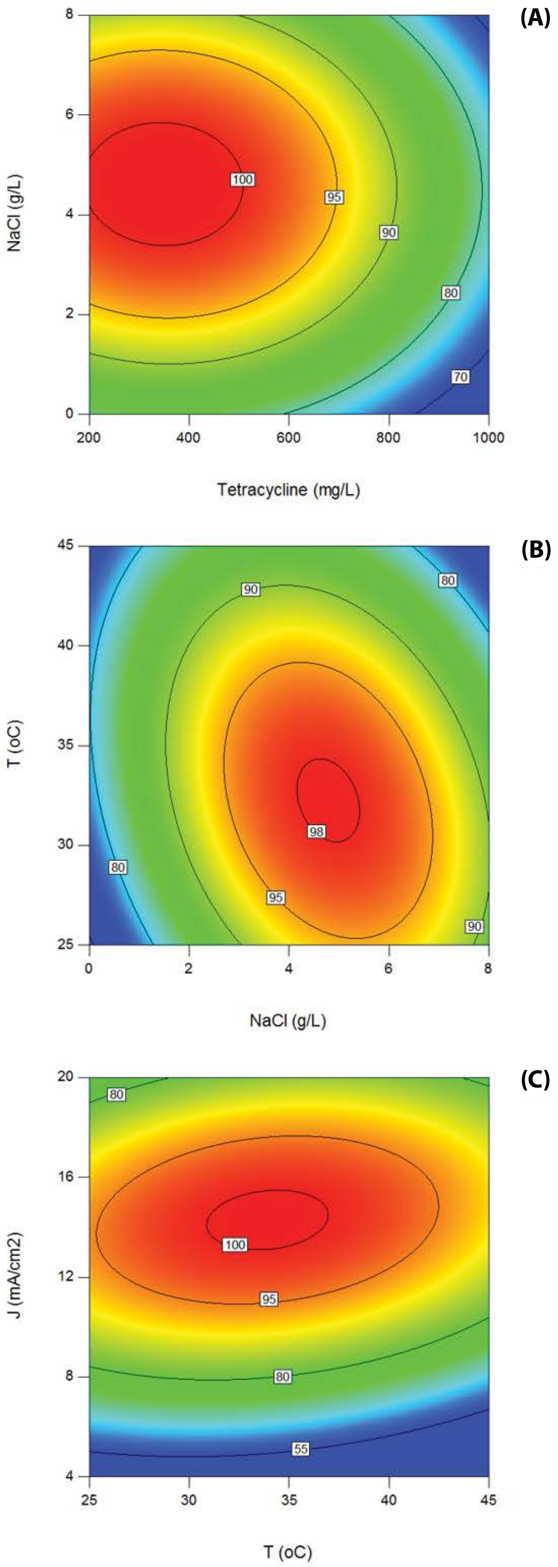

Fig. 7. Effect of parameters on COD removal: (A) effect of tetracycline concentration and NaCl concentration (J = 12 mA/cm^2; T = 35°C), (B) effect of NaCl concentration and reaction temperature ([TCY] = 600 mg/L; J = 12 mA/cm^2), and (C) effect of reaction temperature and current density ([TCY] = 600 mg/L; [NaCl] = 4 g/L).

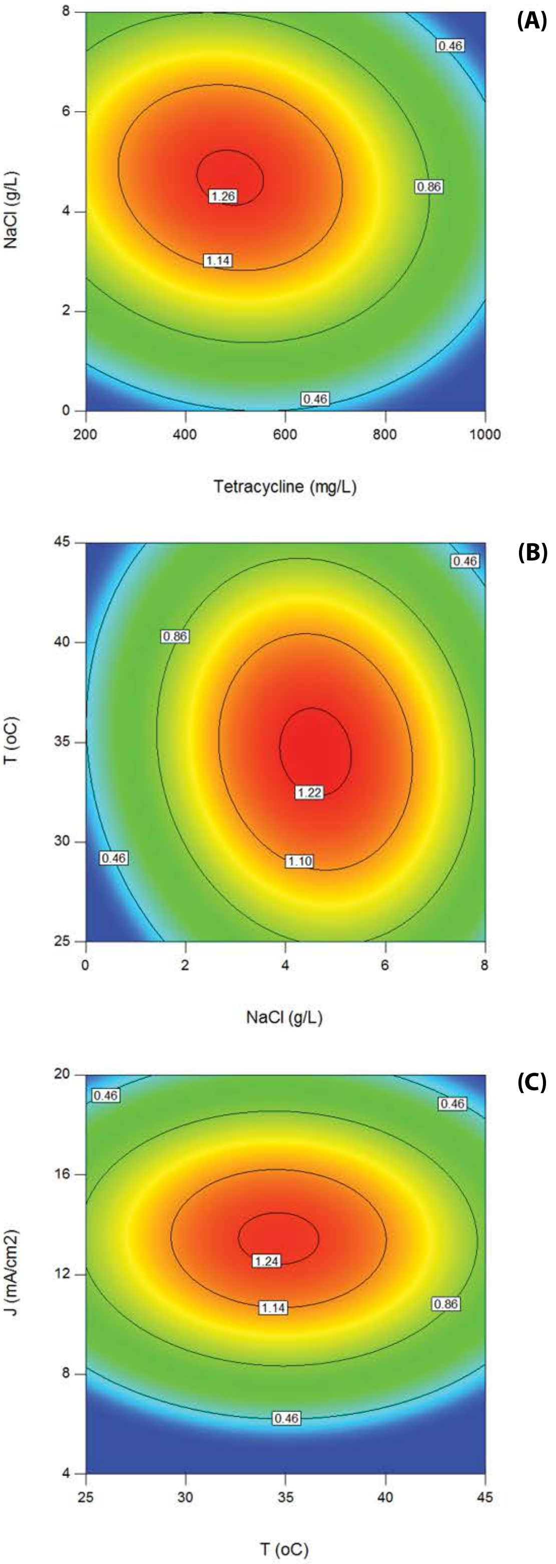

Fig. 8. Effect of parameters on mass transfer coefficient (k_m): (A) effect of tetracycline concentration and NaCl concentration (J = 12 mA/cm^2; T = 35°C), (B) effect of NaCl concentration and reaction temperature ([TCY] = 600 mg/L; J = 12 mA/cm^2), and (C) effect of reaction temperature and current density ([TCY] = 600 mg/L; [NaCl] = 4 g/L).

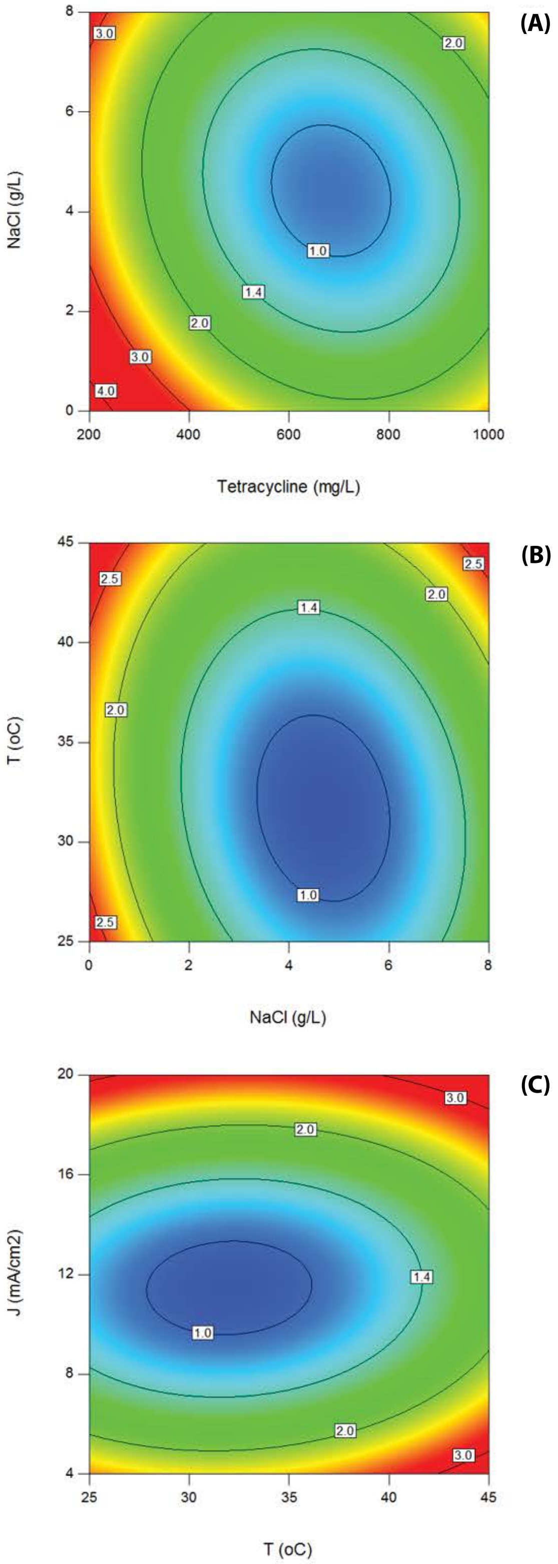

Fig. 9. Effect of parameters on $J/J^o_{\lim}$ ratio: (A) effect of tetracycline concentration and NaCl concentration (J = 12 mA/cm^2; T = 35°C), (B) effect of NaCl concentration and reaction temperature ([TCY] = 600 mg/L; J = 12 mA/cm^2), and (C) effect of reaction temperature and current density ([TCY] = 600 mg/L; [NaCl] = 4 g/L).

In order to optimize the electrochemical process for energy efficient, the energy consumption values were calculated between 37.35–244.20 kWh/kg COD_r with standard deviation of 47.74 kWh/kg COD_r using Eq. (19).

$$EC = \frac{iV_m \Delta t}{\left(COD_o - COD_t\right)V_R} \tag{19}$$

Energy consumption was decreased with increasing NaCl concentration and tetracycline concentration while decreasing the current density in Fig. 10. The reaction temperature was not effective on energy consumption. In Fig. 10, energy consumption smaller than 95 kWh/kg COD_r were obtained at all reaction temperatures in the regions between 1.6–7.9 g/L NaCl concentration, >430 mg/L tetracycline concentration, and <14.9 mA/cm^2 current density.

One of the main objectives of this study was to determine the optimum values of the parameters for process efficiency maximization with minimum energy consumption. In our study, the optimization criteria were applied so that tetracycline removal and COD removal would be maximized whereas EOX and energy consumption would be minimized as outlined in Table 3. Based on the objective of the optimization phase, the importance of COD removal and energy consumption was set as "++++" (more critical) and others were left as "+++" (medium critical) with lower weight and upper weight of "1". In optimization module of Design-Expert software, importance ranges from + to +++++ that specifies the relative importance of one goal vs. another. Weight values range from 0.10 to 10, whereas low weight (0.10) allow more solutions, and high weight (10) cause the optimization to seek a solution close to or beyond the stated goal [55].

In this concept, the optimum values of the parameters were obtained as tetracycline concentration, 618 mg/L; NaCl concentration, 3.6 g/L; current density, 13.4 mA/cm^2; and reaction temperature, 36°C. The optimum values of this study were found similar as in our previous studies for the electrochemical degradation of ampicillin and sulfadiazine antibiotics using BDD electrodes [22,23]. This behavior could be attributed to the mass transfer limitations, reaction rate, and reaction kinetics on the electrochemical degradation of pharmaceutical residues via production of $^{\bullet}OH$ radicals at boron-doped diamond anode and generation of $HOCl/OCl^-$ oxidants in the bulk phase. In Fig. 11, the shaded region indicates the process efficiency for mass transfer-controlled process with tetracycline removal >99%, COD removal >90%, energy consumption <95 kWh/kg COD_r, and pH values 6.0–7.5.

In Table 4, the experimental results of the run at optimum conditions were compared with the values obtained from response surface models for model validation. The relative error values indicated that the relationships obtained between the parameters and the responses were in very good agreement for the electrochemical degradation of tetracycline antibiotic with BDD electrodes. The removal efficiencies of tetracycline, COD, and intermediates at optimum conditions can be seen in Fig. 12. The amount of the reaction intermediates reached a maximum in 20 min and then further oxidized in 120 min. In Fig. 12, the removal efficiencies of tetracycline, COD, and intermediates were

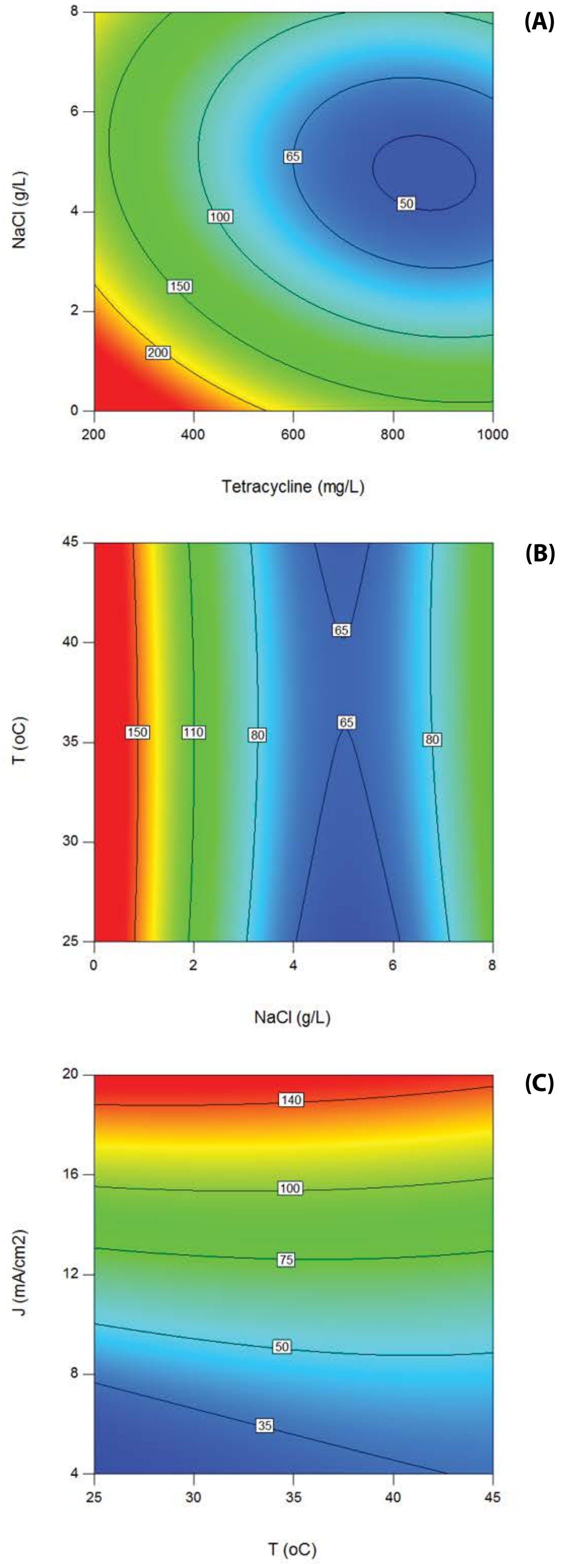

Fig. 10. Effect of parameters on energy consumption: (A) effect of tetracycline concentration and NaCl concentration (J = 12 mA/cm^2; T = 35°C), (B) effect of NaCl concentration and reaction temperature ([TCY] = 600 mg/L; J = 12 mA/cm^2), and (C) effect of reaction temperature and current density ([TCY] = 600 mg/L; [NaCl] = 4 g/L).

Table 3
Optimization criteria applied for the electrochemical degradation of tetracycline antibiotic with BDD electrodes

Parameter	Goal	Lower limit	Upper limit	Lower weight	Upper weight	Importance
Tetracycline concentration (mg/L)	in range	200	1,000	1	1	+++
NaCl concentration (g/L)	in range	0	8	1	1	+++
Current density (mA/cm^2)	in range	4	20	1	1	+++
Reaction temperature (°C)	in range	25	45	1	1	+++
Tetracycline removal (%)	maximize	90	100	1	1	+++
EOX	minimize	0.0000	0.2566	1	1	+++
COD removal (%)	maximize	80	100	1	1	++++
Energy consumption (kWh/kg COD removed)	minimize	37.3	348.8	1	1	++++
pH	in range	6.50	7.50	1	1	+++
Cell voltage (mean) (V)	in range	2.5	30.0	1	1	+++

Table 4
Comparative results of the run at optimum conditions for the electrochemical degradation of tetracycline antibiotic with BDD electrodes ([TCY] = 618 mg/L; J = 13.4 mA/cm^2; [NaCl] = 3.6 g/L; T = 36°C; t = 120 min)

Parameter	Experimental result	RSM model	Error (±%)
Tetracycline removal (%)	98.7	99.6	0.9
EOX	0.1464	0.1307	10.7
COD removal (%)	98.2	99.1	0.9
k_m (m/s)	1.286×10^{-5}	1.214×10^{-5}	5.6
J/J^o_{lim}	>1 (mass transfer-controlled)	>1 (mass transfer-controlled)	–
Energy consumption (kWh/kg COD removed)	78.0	83.8	7.4
pH	7.9	7.5	5.1
Cell voltage (mean) (V)	5.8	6.1	5.2

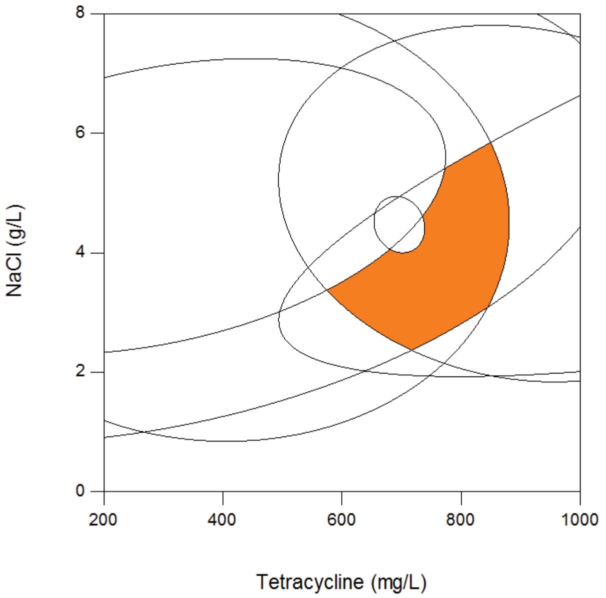

Fig. 11. Optimum operating region for the highest electrochemical degradation efficiency of tetracycline antibiotic with BDD electrodes for tetracycline removal >99%; COD removal >90%; $J/J^o_{\text{lim}} > 1$; $6.0 < \text{pH} < 7.5$; energy consumption <95 kWh/kg COD removed (J = 13.4 mA/cm^2; T = 36°C; t = 120 min).

obtained as 98.7%, 98.2%, and 92.5%, respectively, with 78 kWh/kg COD$_r$ energy consumption. The remaining recalcitrant intermediates could be more resistant to degradation and their very low concentrations may hinder mass transfer for further oxidation.

4. Conclusion

Electrochemical degradation of tetracycline antibiotic with BDD electrodes and the effect of parameters on removal of reaction intermediates was investigated in a batch system. The experimental data were evaluated using response surface methodology. The relationships obtained between the parameters and the responses were in very good agreement according to ANOVA results. The following conclusions were drawn based on the findings of this study:

- Depending on operating conditions; tetracycline removal and COD removal were obtained between 87.3%–100.0% and 49.7%–99.2%, respectively.
- In order to determine the average quantification of intermediates even without the identification of the degradation products, EOX parameter was used with component mass balance in HPLC chromatograms. Intermediates formed with the degradation of tetracycline antibiotic,

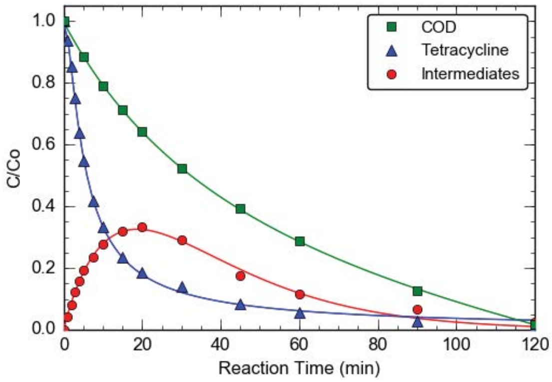

Fig. 12. Removal efficiencies of tetracycline, COD, and intermediates at optimum conditions for the electrochemical degradation of tetracycline antibiotic with BDD electrodes ([TCY] = 618 mg/L; $J = 13.4$ mA/cm^2; [NaCl] = 3.6 g/L; $T = 36$°C; $t = 120$ min).

then further oxidized and removed in high extent (≥97%) depending on reaction conditions.

- Electrochemical process was optimized for the operation in mass transfer-controlled region ($J/J^o_{\lim} > 1$). Optimum values of the parameters were determined as [TCY] = 618 mg/L, [NaCl] = 3.6 g/L, J = 13.4 mA/cm^2 and $T = 36$°C for mass transfer-controlled process.
- Removal efficiencies of tetracycline, COD, and intermediates were obtained as 98.7%, 98.2%, and 92.5%, respectively, with 78 kWh/kg COD$_r$ energy consumption at optimum conditions.

The results of this study indicated the suitability of electrochemical method in the treatment of tetracycline antibiotic that could be found in water and wastewater. The electrochemical reactor equipped with BDD electrode could be operated efficiently as an oxidation and a detoxification stage in the treatment of antibiotics and pharmaceutical residues.

Acknowledgements

The authors gratefully acknowledge TÜBİTAK (The Scientific and Technological Research Council of Turkey) and Mersin University for the financial support. This study was supported by TÜBİTAK with Grant No. 111M341. MSc dissertation was supported by Mersin University Scientific Research Projects Center (MEÜ BAP) with Grant No. BAP-FBE KM (SA) 2011-2 YL.

Symbols and abbreviations

A_e	—	Electrode area, m^2
ANOVA	—	Analysis of variance
BDD	—	Boron-doped diamond
C_0	—	Total area of HPLC chromatogram at initial time ($t = 0$)
$C(t)$	—	Area of HPLC chromatogram of intermediates and by-products at time t
CCD	—	Central composite design
COD	—	Chemical oxygen demand, mg/L
COD$_o$	—	Initial chemical oxygen demand, mg/L
COD$_r$	—	COD removed
DF	—	Degrees of freedom
EC	—	Energy consumption, kWh/kg COD$_r$
EOX	—	Average quantification of electrochemical oxidation intermediates and by-products
F	—	Faraday constant, 96,485 C/mol
J	—	Current density, mA/cm^2
$J^o_{\lim}$	—	Initial limiting current density, mA/cm^2
k	—	Number of parameters
k_m	—	Mass transfer coefficient, m/s
MS	—	Mean square
R^2	—	Regression coefficient
R^2_{adj}	—	Adjusted regression coefficient
RSM	—	Response surface methodology
SS	—	Sum of squares
t	—	Reaction time, min
T	—	Reaction temperature, °C
TCY	—	Tetracycline
V_m	—	Cell voltage (mean), V
V_R	—	Electrolyte volume or reaction volume, mL
x_i, x_j	—	Parameters (factors) (A, B, C and D in the text)
x_{SBER}	—	Fractional COD conversion in stirred batch electrochemical reactor
y	—	Predicted value of the model (response)

Greek

β_0, β_i, β_{ii}, β_{ij}	—	Constant, linear, quadratic, and interaction coefficients in the model
η	—	Response
Δt	—	Reaction time, min
τ_R	—	Total reaction time in stirred batch electrochemical reactor, min

References

[1] K. Kümmerer, Antibiotics in the aquatic environment – a review – Part I, Chemosphere, 75 (2009) 417–434.
[2] V. Homem, L. Santos, Degradation and removal methods of antibiotics from aqueous matrices – a review, J. Environ. Manage., 92 (2011) 2304–2347.
[3] W. Xu, G. Zhang, S. Zou, X. Li, Y. Liu, Determination of selected antibiotics in the Victoria Harbour and the Pearl River, South China using high-performance liquid chromatography-electrospray ionization tandem mass spectrometry, Environ. Pollut., 145 (2007) 672–679.
[4] R. Daghrir, Drogui, Tetracycline antibiotics in the environment: a review, Environ. Chem. Lett., 11 (2013) 209–227.
[5] M. Klavarioti, D. Mantzavinos, D. Kassinos, Removal of residual pharmaceuticals from aqueous systems by advanced oxidation processes, Environ. Int., 35 (2009) 402–417.
[6] B. Halling-Sørensen, Algal toxicity of antibacterial agents used in intensive farming, Chemosphere, 40 (2000) 731–739.
[7] D. Xu, Y. Xiao, H. Pan, Y. Mei, Toxic effects of tetracycline and its degradation products on freshwater green algae, Ecotoxicol. Environ. Saf., 174 (2019) 43–47.
[8] J. Wang, D. Zhi, H. Zhou, X. He, D. Zhang, Evaluating tetracycline degradation pathway and intermediate toxicity during the electrochemical oxidation over a Ti/Ti$_4$O$_7$ anode, Water Res., 137 (2018) 324–334.
[9] I. Sirés, E. Brillas, Remediation of water pollution caused by pharmaceutical residues based on electrochemical separation and degradation technologies: a review, Environ. Int., 40 (2012) 212–229.
[10] A. Kraft, M. Stadelmann, M. Blaschke, Anodic oxidation with doped diamond electrodes: a new advanced oxidation process, J. Hazard. Mater., 103 (2003) 247–261.

[11] M. Miyata, I. Ihara, G. Yoshid, K. Toyod, K. Umetsu, Electrochemical oxidation of tetracycline antibiotics using a Ti/IrO$_2$ anode for wastewater treatment of animal husbandry, Water Sci. Technol., 63 (2011) 456–461.

[12] A. Rossi, V.A. Alves, L.A. Da Silva, M.A. Oliveira, D.O.S. Assis, F.A. Santos, R.R.S. De Miranda, Electrooxidation and inhibition of the antibacterial activity of oxytetracycline hydrochloride using a RuO$_2$ electrode, J. Appl. Electrochem., 39 (2009) 329–337.

[13] D. Belkheiri, F. Fourcade, F. Geneste, D. Floner, H. Aït-Amar, A. Amrane, Feasibility of an electrochemical pre-treatment prior to a biological treatment for tetracycline removal, Sep. Purif. Technol., 83 (2011) 151–156.

[14] C.A. Martínez-Huitle, L.S. Andrade, Electrocatalysis in wastewater treatment: recent mechanism advances, Quim. Nova, 34 (2011) 850–858.

[15] M. Panizza, G. Cerisola, Direct and mediated anodic oxidation of organic pollutants, Chem. Rev., 109 (2009) 6541–6569.

[16] Ch. Comninellis, G. Chen, Electrochemistry for the Environment, Springer, New York, 2010.

[17] G. Saracco, L. Solarino, R. Aigotti, V. Specchia, M. Maja, Electrochemical oxidation of organic pollutants at low electrolyte concentrations, Electrochim. Acta, 46 (2000) 373–380.

[18] C. Carlesi Jara, D. Fino, V. Specchia, G. Saracco, P. Spinelli, Electrochemical removal of antibiotics from wastewaters, Appl. Catal., B, 70 (2007) 479–487.

[19] M. Panizza, C. Bocca, G. Cerisola, Electrochemical treatment of wastewater containing polyaromatic organic pollutants, Water Res., 34 (2000) 2601–2605.

[20] C.I. Brinzila, M.J. Pacheco, L. Ciríaco, R.C. Ciobanu, A. Lopes, Electrodegradation of tetracycline on BDD anode, Chem. Eng. J., 209 (2012) 54–61.

[21] J. Wu, H. Zhang, N. Oturan, Y. Wang, L. Chen, M.A. Oturan, Application of response surface methodology to the removal of the antibiotic tetracycline by electrochemical process using carbon-felt cathode and DSA (Ti/RuO$_2$-IrO$_2$) anode, Chemosphere, 87 (2012) 614–620.

[22] B.K. Körbahti, S. Taşyürek, Electrochemical oxidation of ampicillin antibiotic at boron-doped diamond electrodes and process optimization using response surface methodology, Environ. Sci. Pollut. Res., 22 (2015) 3265–3278.

[23] B.K. Körbahti, S. Taşyürek, Electrochemical oxidation of sulfadiazine antibiotic using boron-doped diamond anode: application of response surface methodology for process optimization, Desal. Water. Treat., 57 (2016) 2522–2533.

[24] X. Chen, G. Chen, F. Gao, P.L. Yue, High-performance Ti/BDD electrodes for pollutant oxidation, Environ. Sci. Technol., 37 (2003) 5021–5026.

[25] M. Panizza, G. Cerisola, Application of diamond electrodes to electrochemical processes, Electrochim. Acta, 51 (2005) 191–199.

[26] E. Weiss, K. Groenen-Serrano, A. Savall, A comparison of electrochemical degradation of phenol on boron doped diamond and lead dioxide anodes, J. Appl. Electrochem., 38 (2008) 329–337.

[27] Ch. Comninellis, A. Kapalka, S. Malato, S.A. Parsons, I. Poulios, D. Mantzavinos, Advanced oxidation processes for water treatment: advances and trends for R&D, J. Chem. Technol. Biotechnol., 83 (2008) 769–776.

[28] E. Brillas, C.A. Martínez-Huitle, Decontamination of wastewaters containing synthetic organic dyes by electrochemical methods. An updated review, Appl. Catal., B, 166–167 (2015) 603–643.

[29] B. Marselli, J. Garcia-Gomez, P.A. Michaud, M.A. Rodrigo, Ch. Comninellis, Electrogeneration of hydroxyl radicals on boron-doped diamond electrodes, J. Electrochem. Soc., 150 (2003) D79, doi: 10.1149/1.1553790.

[30] D. Zhi, J. Qin, H. Zhou, J. Wang, S. Yang, Removal of tetracycline by electrochemical oxidation using a Ti/SnO$_2$-Sb anode: characterization, kinetics, and degradation pathway, J. Appl. Electrochem., 47 (2017) 1313–1322.

[31] B.K. Körbahti, Response surface optimization of electrochemical treatment of textile dye wastewater, J. Hazard. Mater., 145 (2007) 277–286.

[32] G. Tchobanoglous, F. Burton, H. Stensel, Wastewater Engineering, Treatment and Reuse, McGraw-Hill, New York, 2004.

[33] B.K. Körbahti, A. Tanyolaç, Continuous electrochemical treatment of simulated industrial textile wastewater from industrial components in a tubular reactor, J. Hazard. Mater., 170 (2009) 771–778.

[34] B.K. Körbahti, K. Artut, Electrochemical oil/water demulsification and purification of bilge water using Pt/Ir electrodes, Desalination, 258 (2010) 219–228.

[35] B.K. Körbahti, K. Artut, Bilge water treatment in an upflow electrochemical reactor using Pt anode, Sep. Sci. Technol., 48 (2013) 2204–2216.

[36] E.R. Burns, C. Marshall, Correction for chloride interference in the chemical oxygen demand test, Water Environ. Res., 37 (1965) 1716–1721.

[37] F.J. Baumann, Dichromate reflux chemical oxygen demand: a proposed method for chloride correction in highly saline wastes, Anal. Chem., 46 (1974) 1336–1338.

[38] D.C. Montgomery, Design and Analysis of Experiments, John Wiley & Sons, New Jersey, 2009.

[39] R.H. Myers, D.C. Montgomery, C.M. Andersen-Cook, Response Surface Methodology: Process and Product Optimization using Designed Experiments, John Wiley & Sons, New Jersey, 2009.

[40] Stat-Ease, Inc., Handbook for Experimenters, Minnesota, 2021.

[41] M.J. Anderson, P.J. Whitcomb, DOE Simplified: Practical Tools for Effective Experimentation, CRC Press, New York, 2007.

[42] Z.M. Shen, D. Wu, J. Yang, T. Yuan, W.H. Wang, J.P. Jia, Methods to improve electrochemical treatment effect of dye wastewater, J. Hazard. Mater. B, 131 (2006) 90–97.

[43] I. Dalmázio, M.O. Almeida, R. Augusti, T.M.A. Alves, Monitoring the degradation of tetracycline by ozone in aqueous medium via atmospheric pressure ionization mass spectrometry, J. Am. Soc. Mass Spectrom., 18 (2007) 679–687.

[44] H. Zhang, F. Liu, X. Wu, J. Zhang, D. Zhang, Degradation of tetracycline in aqueous medium by electrochemical method, Asia-Pac. J. Chem. Eng., 4 (2009) 568–573.

[45] M.D. Vedenyapina, Y.N. Eremicheva, V.A. Pavlov, A.A. Vedenyapin, Electrochemical degradation of tetracycline, Russ. J. Appl. Chem., 81 (2008) 800–802.

[46] X.D. Zhu, Y.J. Wang, R.J. Sun, D.M. Zhou, Photocatalytic degradation of tetracycline in aqueous solution by nanosized TiO$_2$, Chemosphere, 92 (2013) 925–932.

[47] Y. Zhang, J. Zhou, X. Chen, L. Wang, W. Cai, Coupling of heterogeneous advanced oxidation processes and photocatalysis in efficient degradation of tetracycline hydrochloride by Fe-based MOFs: synergistic effect and degradation pathway, Chem. Eng. J., 369 (2019) 745–757.

[48] T. Luo, H. Feng, L. Tang, Y. Lu, W. Tang, S. Chen, J. Yu, Q. Xie, X. Ouyang, Z. Chen, Efficient degradation of tetracycline by heterogeneous electro-Fenton process using Cu-doped Fe@Fe$_2$O$_3$: mechanism and degradation pathway, Chem. Eng. J., 382 (2020) 122970, doi: 10.1016/j.cej.2019.122970.

[49] R. Bellagamba, P. Michaud, Ch. Comninellis, N. Vatistas, Electro-combustion of polyacrylates with boron-doped diamond anodes, Electrochem. Commun., 4 (2002) 171–176.

[50] B. Louhichi, M.F. Ahmadi, N. Bensalah, A. Gadri, M.A. Rodrigo, Electrochemical degradation of an anionic surfactant on boron-doped diamond anodes, J. Hazard. Mater., 158 (2008) 430–437.

[51] T. González, J.R. Domínguez, P. Palo, J. Sánchez-Martín, E.M. Cuerda-Correa, Development and optimization of the BDD-electrochemical oxidation of the antibiotic trimethoprim in aqueous solution, Desalination, 280 (2011) 197–202.

[52] B.K. Körbahti, P. Demirbüken, Electrochemical oxidation of resorcinol in aqueous medium using boron-doped diamond anode: reaction kinetics and process optimization with response surface methodology, Front. Chem., 5 (2017) 75, doi: 10.3389/fchem.2017.00075.

[53] D. Pletcher, F.C. Walsh, Industrial Electrochemistry, Chapman and Hall, New York, 1990.

[54] K. Rajeshwar, J.G. Ibanez, Environmental Electrochemistry, Academic Press, New York, 1997.

[55] M.J. Anderson, P.J. Whitcomb, RSM Simplified: Optimizing Processes Using Response Surface Methods for Design of Experiments, CRC Press, New York, 2005.